

STRUCTURAL ANALYSIS OF POLYMERIC FOAMS BY SUB- μM X-RAY COMPUTED TOMOGRAPHY

Johann KASTNER, Richard KICKINGER, Dietmar SALABERGER
Upper Austria University of Applied Sciences, Wels Campus, A - 4600, Austria

Abstract

Due to the light weight, excellent strength/weight ratio, superior thermal and acoustic insulation properties polymeric foams are the material of choice for many applications. They can be found in many products of daily life like cars and mattresses. The main fields of applications are packaging, automotive industry, leisure- and furniture industry as well as construction. Foams can be classified in closed and open cell materials. Within this paper we have investigated different kinds of polymeric foams and in particular foam with embedded cellulose particles - a new material for special mattresses. These materials were characterized by cone beam high resolution X-ray computed tomography (CT) with resolutions between 0.7 μm and 10 μm . In order to get enough contrast the CT-measurements were performed with tube voltages below 50 kV. The CT-data was processed by various algorithmic steps (e.g. denoising, thresholding, watershed transformation, erosion) to get the open or closed cell structure in 3 dimensions. Finally, the following characteristic data was deduced from the CT-results:

- Position, diameter, shape and volume of all cells, total number of cells, average cells per mm^3
- Position of all polymeric nodes, total number of nodes and average nodes per mm^3 and average nodes per cell
- Position, diameter, shape and volume of all cellulose particles, total number of particles and average particles per mm^3
- Average particles per cell and fraction of nodes containing particles
- Nature of nodes concerning the number of branches (tetrahedral, hexahedral or other)
- Distances between nodes and particles.

1. Introduction

Polymeric foams are important materials for many applications in life sciences, leisure- and furniture industry as well as construction. Foams can be found in e.g. light-weight structures and mattresses [1]. The physical properties like strength/weight ratio, thermal and acoustic insulation and potential applications of foams result from the chemistry and physical properties of the bulk material and the cell structure of the foams [1, 2].

Foam characterization is usually performed using visual inspection, optical microscopy and confocal microscopy [2, 3]. In particular, microscopic techniques can be used to measure many features, including window thickness, cell diameters and strut lengths. However, because of the complicated three-dimensional structures of foams, measuring foam features manually is time consuming, and often requires destruction of the sample since these methods give only information about the foam surface [2, 3]. In addition, some distinguishing features of foams, including cell volume, are extremely difficult to measure at all using traditional techniques, since information of

the inner structure is necessary. Cone beam X-ray computed tomography is a non-destructive method, which is appropriate for characterisation of polymeric foams [3, 4], since a complete 3D-information of the inner structure is generated.

Within this paper we have investigated closed cell polypropylene foam and in particular an open cell polyurethane foam with embedded cellulose particles - a new material for special mattresses - by a X-ray based non-destructive method. The foams were characterized by cone beam high resolution X-ray computed tomography (CT) and physical parameters for the cells, nodes and particles were determined quantitatively.

2. Experimental

Samples

Two kinds of foams were investigated; a polypropylene (PP) foam with closed cells and an open cell polyurethane (PUR) foam with cellulose particles called cellpur. These foams are used for automotive and furniture industry.

Computed Tomography

a.) CT-data Recording

The CT X-ray tomograms were scanned using a Nanotom 180NF CT device developed and manufactured by GE Sensing & Inspection Technologies phoenix|x-ray with a 180 keV high power nanofocus tube and a 2300x2300 pixel Hamamatsu detector. Targets made of Molybdenum were used. The voxel sizes used were between 0.7 and 10 μm , the voltage at the nano-focus tube was 40-50 kV. An overview of the measurement parameters can be found in table 1.

Table 1. Overview of the samples investigated and the corresponding CT-measurement parameters. PP=polypropylene, PUR=polyurethane.

Material	Foam	Voxel size [μm]	U [kV]	I [μA]	Projections	Measurement time [min]
PP	Closed	3.6	49	198	1500	120
PUR with particles, sample1	Open	2.2	50	200	1500	122
PUR with particles, sample1	Open	0.7	50	450	1700	283
PUR with particles, sample2	Open	10	40	400	1500	112

a.) CT-data Evaluation

The cone beam CT-data was reconstructed by means of a filtered back projection Feldkamp-algorithm. The reconstructed CT-data was visualised and processed with the software VGStudio MAX 2.0 by Volume Graphics GmbH [5]. For cell characterisation MAVI (Modular Algorithms for Volume Images) [6] was used. The CT-data was evaluated by the following steps: binarisation by thresholding, denoising by Median filter, foam reconstruction by preflooded watershed-algorithm,

calculation of the cell features. The data relating to the size, shape, volume and position of the cells was generated and extracted for use in further analysis.

For combined cell, node and particle characterisation both VGStudio MAX 2.0 and MAVI were used. For extraction of the particle data-set a thresholding algorithm and for extraction of node data-set an erosion algorithm was used. The registered cell, particle and node data was evaluated by a Matlab code so that the following features could be determined:

- Position, diameter, shape and volume of all cells, total number of cells, average cells per mm^3
- Position of all polymeric nodes, total number of nodes and average nodes per mm^3 and average nodes per cell
- Position, diameter, shape and volume of all cellulose particles, total number of particles and average particles per mm^3
- Average particles per cell and fraction of nodes containing particles
- Nature of nodes concerning the number of branches (tetrahedral, hexahedral or other)
- Distances between nodes and particles.

3. Results and Discussion

Figure 1 shows a cross-sectional CT picture of a polypropylene foam granule. As figure 1 clearly shows it is closed cell foam. With the high CT-resolution all the individual walls are clearly visible, and show/have thicknesses in the range between 8 and 15 μm .

Fig. 2 shows a cross-section and a 3D-picture of the CT-results of polymeric foam with cellulose particles. The 3D-structure of this open cell foam as well as the individual cellulose particles embedded in the polymeric walls are clearly visible. As Fig. 2. shows the cellulose particles are mostly embedded in the wall crossings, this means at the polymer nodes.

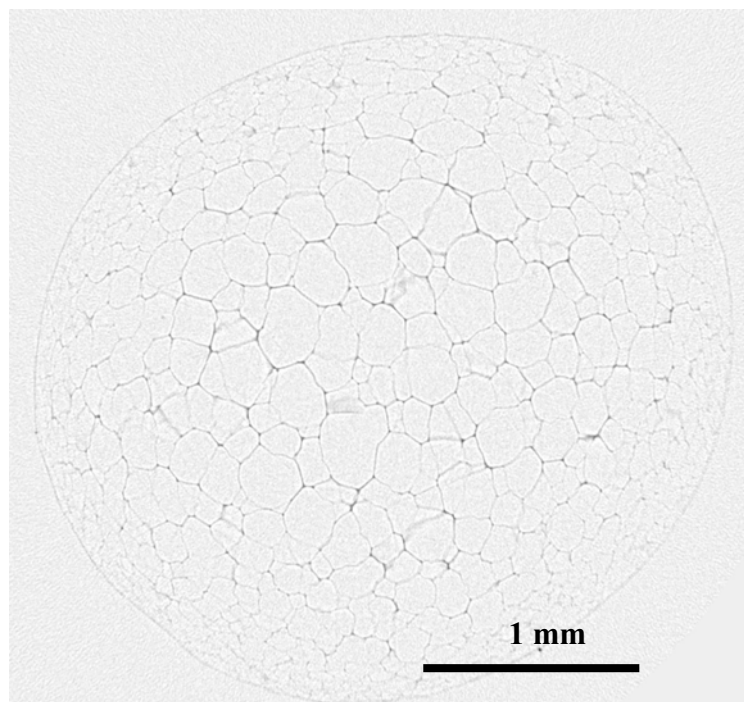


Fig. 1: Cross-sectional CT-picture of polypropylene foam showing the closed cell structure. For presentation the x-ray absorbing polymer is represented in black and the air in white. Voxel size $(3.6 \mu\text{m})^3$

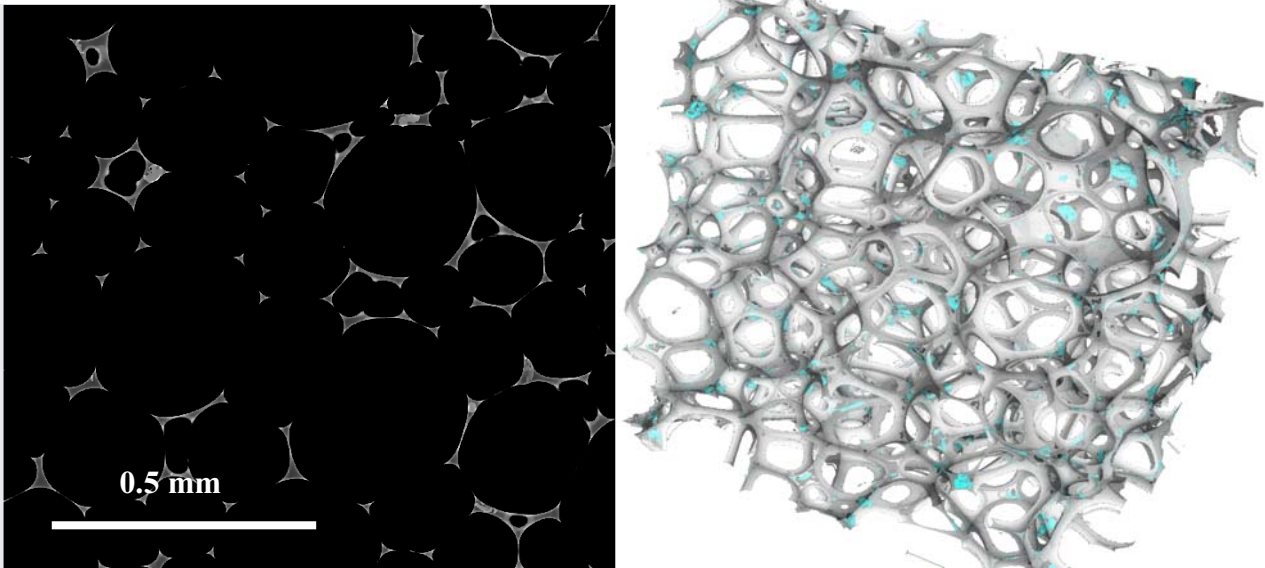


Fig. 2: Cross-sectional CT-picture of a polymeric foam with cellulose particles (left picture). 3-dimensional picture of CT-data of the polymeric foam with cellulose particles visualised by surface rendering (right picture). Both pictures show the open foam structure and the cellulose particles within the polymeric walls. Voxel size $(2.2 \mu\text{m})^3$.

Fig. 3 shows a high resolution cross-sectional CT-picture of the PUR-foam with an embedded cellulose particle measured with a voxel size of $0.7 \mu\text{m}$. The cellulose particle within the polymeric foam is clearly visible and can be separated from the polymeric matrix. Fig. 4 also shows, that the grey value at the polymer-air interface is much higher than within the polymer. This can be explained by a rather strong phase contrast effect caused by the small focal spot size and the high resolution of the CT-measurement.

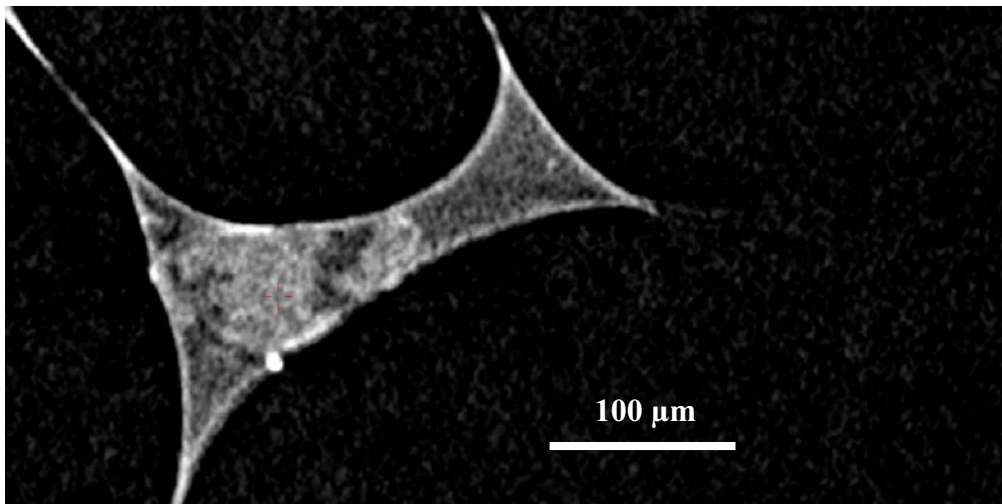


Fig. 3: High resolution cross-sectional CT-picture of a polymeric foam with cellulose particles. Voxel size $(0.7 \mu\text{m})^3$.

The CT-data was further processed by various image processing methods like filtering, thresholding and watershed transformation as described in chapter 2. In this way characteristic data of both open and closed cell structures could be determined. Figure 4 shows the cell diameter distribution of two PUR-samples with cellulose particles. It can be seen that for both samples the distribution functions look more or less Gaussian or better or more correctly like a Weibull function. An easy Gauss fit gives a mean diameter of $465 \mu\text{m}$ and a standard deviation of $195 \mu\text{m}$ for sample 1 and a mean diameter of $395 \mu\text{m}$ with a standard deviation of about $320 \mu\text{m}$ for sample 2.

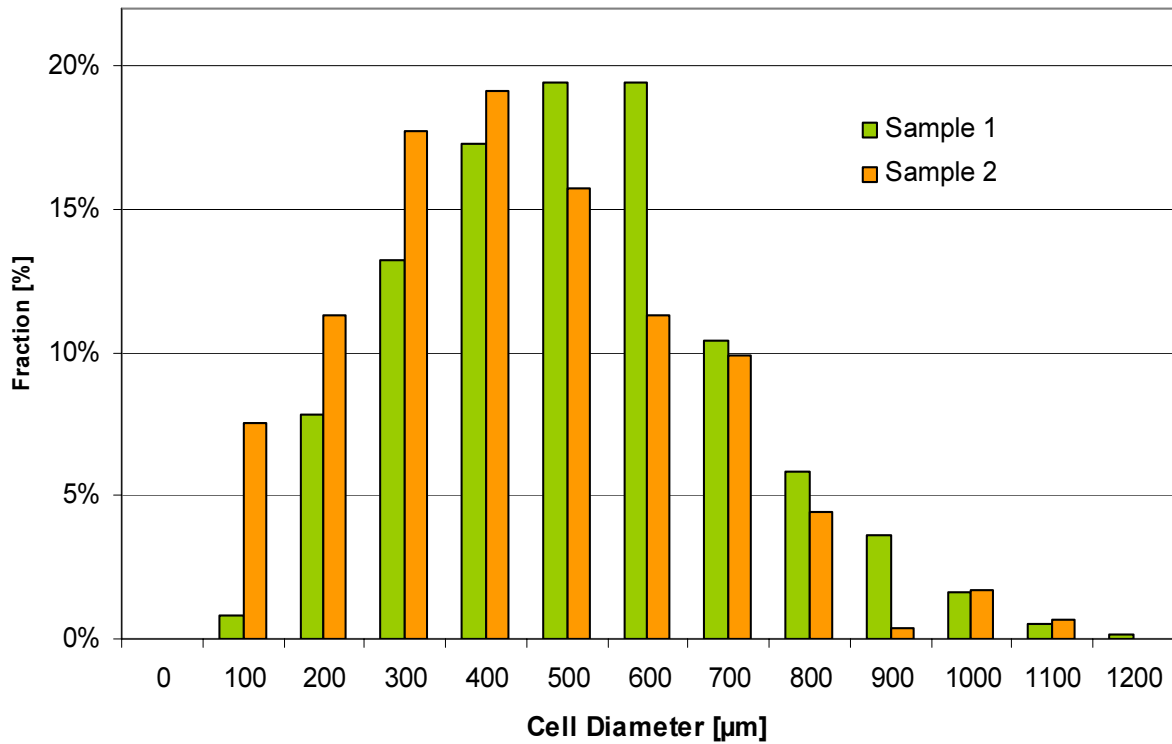


Fig. 4: Cell diameter distribution of the PUR-samples with cellulose particles for two samples. Sample 1 was scanned with a voxel size of $(2.2 \mu\text{m})^3$ and sample 2 with $(10 \mu\text{m})^3$.

In Fig. 5 the cellulose particle diameter distribution of the PUR-sample is presented; due to the limited CT-resolution particles with a diameter below $10 \mu\text{m}$ were neglected. It can be seen that the maximum of the distribution function is below $20 \mu\text{m}$ and the particle diameter reaches values up to $100 \mu\text{m}$.

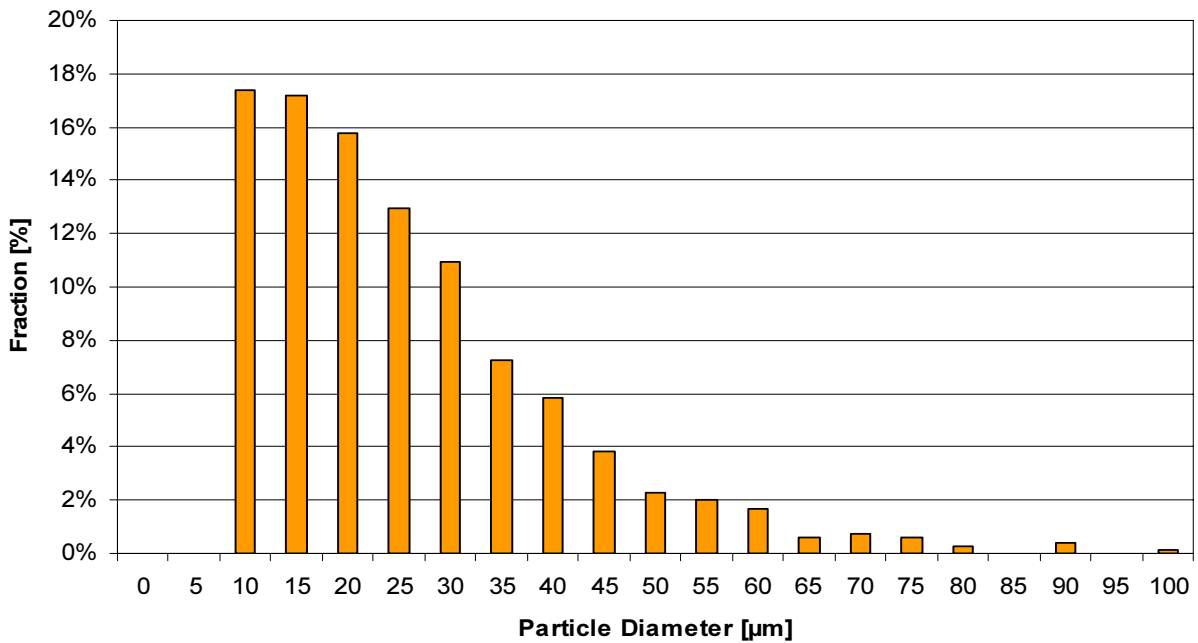


Fig. 5: Cellulose particle distribution of the PUR-samples with cellulose particles. The results were determined from the CT-data presented in Fig. 2. Diameters below $10 \mu\text{m}$ were not evaluated.

In addition to the cell and particle properties also properties of the polymeric nodes are determined. Mainly two different kinds of nodes – tetrahedral with 4 branches and hexahedral with 8 branches – appear in the sample. Fig. 6 shows 3D-pictures of two typical nodes.

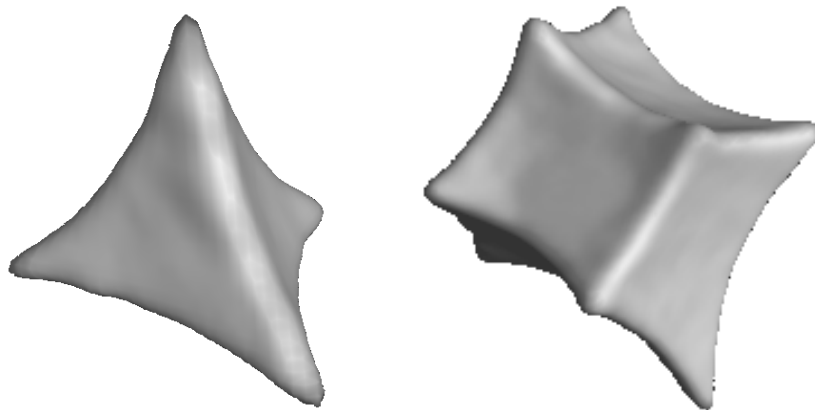


Fig. 6: Shape of two typical polymeric nodes. The left one has four branches (tetrahedral) and the right one has 8 branches (hexahedral).

The characteristic data for the cells, particles and nodes was combined and the interdependences were evaluated as well. Table 2 summarizes the most important features deduced from the CT-data of the PUR-sample with the cellulose particles.

Table 2. Overview of the most important features (cell, node and particle features) deduced for a volume of 19.3 mm³ of the PUR-sample with the cellulose particles.

Feature	Value
Number of cells	292
Average cells per mm ³	15.2
Average diameter of cells	390-470 μm
Number of nodes	1711
Average nodes per mm ³	88.7
Number of particles	787
Average particles per mm ³	41
Average nodes per cell	5.9
Particle diameter	95 % of the particles <60 μm
Average particles per cell	2.7
Fraction of nodes containing particles	46 %
Shape of nodes (number of branches)	Tetrahedral: ~80 % Hexahedral: ~20 % Other shapes: < 3 %

The cellulose particles can be at different positions; most are within polymeric nodes and only a few are outside the nodes. Fig. 7 shows a 3D-rendering of various nodes and cellulose particles. From

the four nodes two are without cellulose particles and two incorporate cellulose particles. On the left side of Fig. 7 there is a spherical particle visible, which is outside the neighbouring node.

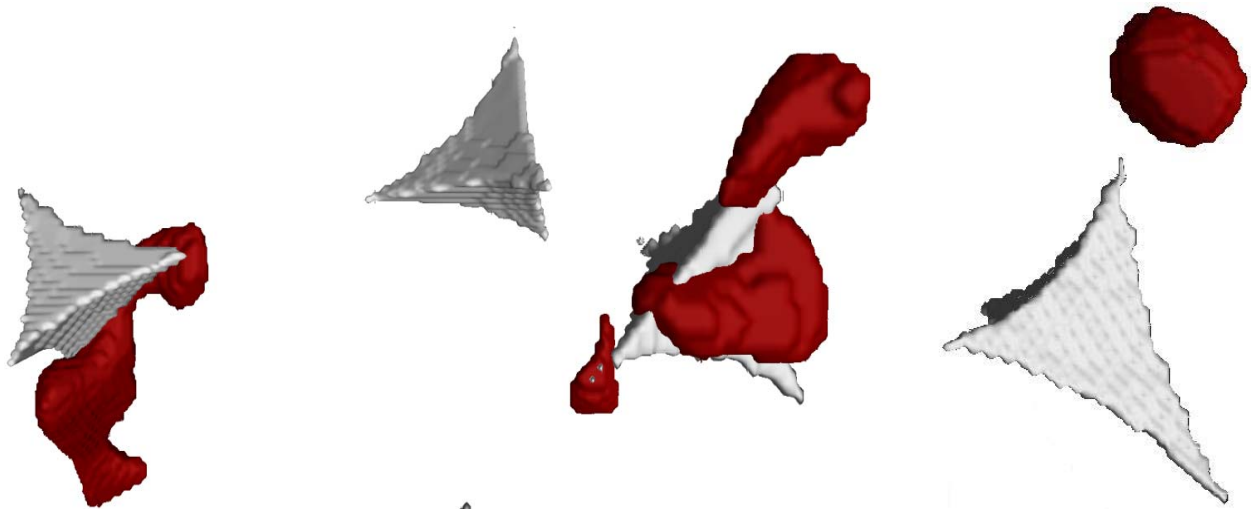


Fig. 7: 3D-rendering of a selected volume of the CT-data for the PUR-sample 1 set showing four polymeric nodes and three cellulose particles. The polymer is represented in grey and the cellulose particles in dark red. The particles are mainly within the nodes, only the cellulose particle at the right side is outside of the polymeric node structure.

A detailed analysis of the position of the cellulose particles in comparison to the polymeric nodes is presented in Fig. 7, where the distribution function for the center-center distance between the cellulose particles and the nodes for the PUR-samples is shown. It can be seen, that the distances between 0 and 200 μm with a maximum are about 30 μm . The distribution function is asymmetric with a steep decline at values below 30 μm and flat decline at high distances.

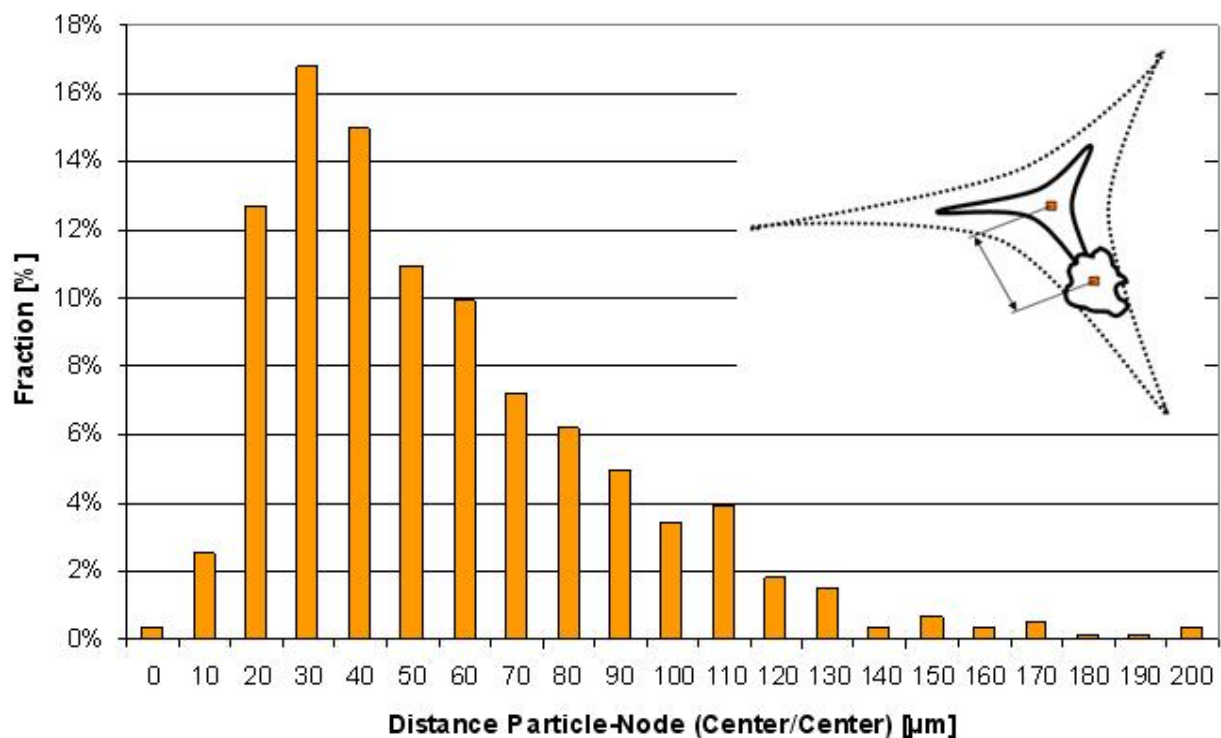


Fig. 8: Distance between the cellulose particles and the nodes for the PUR-samples with cellulose particles. The inset demonstrates how this distance was determined. The results were determined from the CT-data presented in Fig. 2.

4. Summary and conclusion

We have used high-resolution CT with voxel sizes between 2 μm and 10 μm for the characterisation of different polymeric foams with open and closed cell structures as well as for an open cell material with cellulose particles embedded within the walls.

CT is very useful to get high resolution 3-dimensional information about the various foams. For the polymeric foam with cellulose particles the individual cellulose particles within the polymeric walls could be segmented and analysed. The CT-data was analysed by 3D-image processing methods so that the following characteristic data could be derived:

- ✓ Position, diameter, shape and volume of all cells
- ✓ Position of all polymeric nodes, total number of nodes and average nodes per mm^3
- ✓ Position, diameter, shape and volume of all cellulose particles
- ✓ Average particles per cell and fraction of nodes containing particles Nature of nodes concerning the number of branches
- ✓ Distances between nodes and particles

Structural analysis of foams by high-resolution CT is very useful. It enables polymer companies and research institutes to optimise the foam products and the production processes.

Acknowledgement

The project was supported by FHplus in COIN and by the COMET-programme of FFG. We thank Borealis Polyolefine GmbH and Lenzing AG for providing the foam samples.

References

1. Klempner D. and Sendijarevic V.: Polymeric Foams and Foam Technology, München: Carl Hanser Verlag, 2004.
2. Michaeli, W., Tondorf A. and Berdel K.: Three-Dimensional Structural Analysis of foams. *Kunststoffe international* 97 (2007), 174-177.
3. Montminy M. D., Tannenbaum A. R. and Macosko C. W.: The 3D structure of real polymer foams, *Journal of Colloid and Interface Science* 280 (2004), 202–211.
4. Kastner J. (Editor): Proceedings Industrielle Computertomografietagung, Wels, Austria, 26. + 27. February 2008, Aachen: Shaker Verlag, 2008.
5. www.volumegraphics.com
6. www.itwm.fhg.de/bv/projects/MAVI